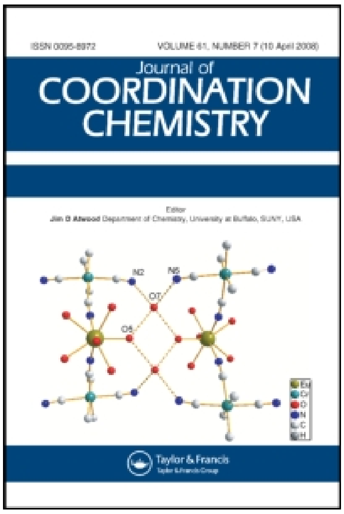

Journal of Coordination Chemistry
Publication details, including instructions for authors and subscription information:
http://www.informaworld.com/smpp/title~content=t713455674

Synthesis and magnetic, spectral and thermal eukaryotic DNA studies of some 2-acetylpyridine- [N-(3-hydroxy-2-naphthoyl)] hydrazone complexes

K. M. Ibrahim[a]; I. M. Gabr[a]; R. R. Zaky[a]
[a] Faculty of Science, Chemistry Department, Mansoura University, Mansoura, Egypt

To cite this Article Ibrahim, K. M. , Gabr, I. M. and Zaky, R. R.(2009) 'Synthesis and magnetic, spectral and thermal eukaryotic DNA studies of some 2-acetylpyridine- [N-(3-hydroxy-2-naphthoyl)] hydrazone complexes', Journal of Coordination Chemistry, 62: 7, 1100 — 1111, First published on: 29 July 2010 (iFirst)

To link to this Article: DOI: 10.1080/00958970802464616

URL: http://dx.doi.org/10.1080/00958970802464616

Journal of Coordination Chemistry
Vol. 62, No. 7, 10 April 2009, 1100–1111

Taylor & Francis
Taylor & Francis Group

Synthesis and magnetic, spectral and thermal eukaryotic DNA studies of some 2-acetylpyridine-[N-(3-hydroxy-2-naphthoyl)] hydrazone complexes

K.M. IBRAHIM, I.M. GABR* and R.R. ZAKY

Faculty of Science, Chemistry Department, Mansoura University,
Mansoura, Egypt

(*Received 22 April 2008; in final form 2 July 2008*)

Complexes of Ni(II), Co(II), Cu(II), Zn(II), Cd(II), Hg(II) and U(VI)O_2 with 2-acetylpyridine-[N-(3-hydroxy-2-naphthoyl)] hydrazone (H_2APHNH) have been prepared and characterized by elemental analysis, molar conductance, thermal (TG, DTG), spectral (^{1}H NMR, IR, UV–Vis, ESR) and magnetic measurements. ^{1}H NMR spectrum of the ligand suggests the presence of intramolecular hydrogen bonding. IR spectra show that H_2APHNH is a bidentate, tridentate and/or tetradentate ligand. Thermal decomposition of some complexes ended with metal oxide as a final product. ESR spectra gave evidence for the proposed structure and the bonding for some Cu(II) complexes. Biological activity measurements were carried out.

Keywords: Hydrazone complexes; ESR; Thermal; Biological activities

1. Introduction

Hydrazones are versatile ligands having biological activities with use as reagents for selective chemical separation of metal ions [1], insecticides, anticoagulants, antitumor agents, antioxidants, plant growth regulators [2], antibacterial, antimicrobial, antineoplastic, antiviral, anti-inflammatory, antileukemic and enzymatic reaction inhibitors [3–7]. Their metal complexes have applications in nonlinear optics, sensors and medicine [8]. Furthermore, hydrazones incorporating heterocyclic moieties exhibit interesting coordinating behavior with transition metal ions [9]. The present work synthesizes and characterizes complexes formed between (H_2APHNH) (figure 1) and Ni(II), Co(II), Cu(II), Zn(II), Cd(II), Hg(II) and U(VI)O_2. The possible modes of chelation, the geometry and the nature of bonding of the complexes are discussed on the basis of various spectroscopic methods.

---

*Corresponding author. Email: issam_gabr@yahoo.com

Journal of Coordination Chemistry
ISSN 0095-8972 print/ISSN 1029-0389 online © 2009 Taylor & Francis
DOI: 10.1080/00958970802464616

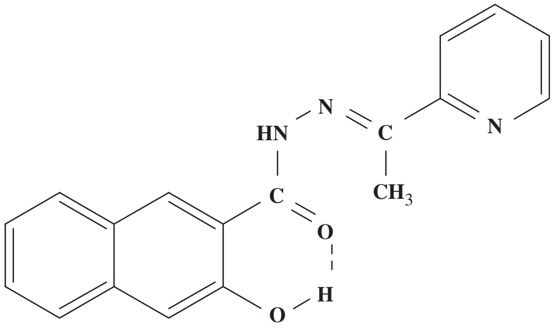

Figure 1. 2-Acetylpyridine-[N-(3-hydroxy-2-naphthoyl)] hydrazone (H_2APHNH).

2. Experimental

2.1. *Apparatus and reagents*

IR absorption spectra were recorded on a Mattson 5000 FTIR spectrophotometer. Electronic spectra were measured on a Unicam UV–Vis spectrometer UV_2. Thermogravimetric analysis was performed using an automatic recording thermobalance (951 DuPont instrument). Samples were heated at a rate of $10^\circ C\,min^{-1}$ (25–800°C) in N_2. ^1H NMR spectrum for H_2APHNH, in d_6-DMSO, was recorded on an EM-390 (200 MHz) spectrometer. Mass spectra were recorded on a Varian MAT 311 spectrometer. Carbon and hydrogen contents for the ligand and complexes were determined at the Microanalytical Unit, Mansoura University, Egypt. Ni(II), Co(II), Cu(II), Zn(II), Cd(II), Hg(II), U(VI)O_2, Cl and SO_4^{2-} contents in the complexes were determined by standard methods [10]. ESR spectra were obtained on a Bruker EMX spectrometer working in the X-band (9.78 GHz) with 100 kHz modulation frequency. The microwave power was set at 1 mW and modulation amplitude was set at 4 Gauss. The low field signal was obtained after 4 scans with a 10-fold increase in the receiver gain. A powder spectrum was obtained in a 2 mm quartz capillary at room temperature. All metal salts used were pure (Fluka, Aldrich or Merck).

2.2. *Preparation of the ligand*

H_2APHNH was prepared by heating under reflux a mixture of 3-hydroxy naphthoic acid hydrazide (0.01 mol, 3.06 g) and 2-acetylpyridine (0.01 mol, 1.21 g) in absolute ethanol for 2 h. On heating, pale yellow crystals were formed, filtered off, washed with ethanol and Et_2O and recrystallized from ethanol (m.p. 245°C; yield 90%). The purity of the compound was checked by TLC.

2.3. *Preparation of complexes*

The metal complexes were prepared by mixing equimolar amounts of metal chlorides or acetates and the ligand in absolute ethanol; aqueous-ethanolic solution was required for $CdSO_4 \cdot H_2O$. The reaction mixture was heated under reflux for 1–3 h depending on the metal salt used. The isolated solid complexes were filtered while the solution was still hot, washed several times with ethanol and diethyl ether, and dried and stored in a vacuum desiccator over anhydrous $CaCl_2$. Two kinds of complexes were obtained using metal chloride or acetate of Ni(II), Co(II), Cu(II) and Zn(II), chloride or sulfate of Cd(II) and one kind using the chloride of Hg(II) and the acetate of $U(VI)O_2$.

2.4. *Biological activity*

2.4.1. Antimicrobial activity. The ligand and complexes were tested as antibacterial agents at the Department of Microbiology, Faculty of Pharmacy, Mansoura University. Seeded agar plates were prepared by putting 50 mL of inoculated agar into 15 cm Petri dishes and allowing them to solidify. Cups were made to receive 25 µl of the solution and allowed to diffuse and incubate at 37°C for 24 h. Inhibition zone was measured [11] and compared with that of gentamicin solution (commercial antibiotic, Memphis Co., Egypt, 1000 $\mu g\,mL^{-1}$). The experiment control was DMSO.

2.4.2. Genotoxicity activity. A solution of 2 mg of calf thymus DNA was dissolved in 1 mL of sterile distilled water. Stock concentrations of the investigated ligand and complexes were prepared by dissolving 2 $mg\,mL^{-1}$ DMSO. An equal volume of each compound and DNA were mixed thoroughly and kept at room temperature for 2–3 h. The effect of the chemicals on the DNA was analyzed by agarose gel electrophoresis. A 2 µL of loading dye was added to 15 µL of the DNA mixture before being loaded into the well of an agarose gel. The loaded mixtures were fractionated by electrophoresis, visualized by UV and photographed.

3. Results and discussion

Elemental analyzes showed different stoichiometries for the isolated metal complexes (table 1) which have high melting points (>300°C), are insoluble in most common solvents but soluble in DMF or DMSO.

3.1. *IR and ^1H NMR spectra*

The ^1H NMR spectrum of H_2APHNH in d_6-DMSO shows signals at 11.68 and 11.79 ppm assignable to (NH) and $(OH)_{naphthoic}$, respectively. The signal attributed to OH at a high value downfield from TMS suggests the presence of intramolecular hydrogen bonding. Multiplet signals observed in the 7.34–8.67 ppm region are assigned to protons of phenyl and napthyl rings. The sharp singlet observed at 2.48 ppm is assigned to methyl protons ($-N{=}C{-}C\underline{H}_3$).

The IR spectrum of H_2APHNH displays bands at 1660, 1640, 610, 1270 and 3261 cm^{-1} assigned to $\upsilon(C{=}O)$ [12], $\upsilon(C{=}N)_{hydrazone}$ [13], $\upsilon(C{=}N)_{pyridine}$ [14], $\upsilon(C{-}O)_{naphthoic}$ [15] and $\upsilon(NH)$ [16], respectively. The presence of $\upsilon(OH)$ as a broad band at low wavenumber 3343 cm^{-1} as well as the broad weak bands in the 1950–2080 and 2150–2240 cm^{-1} regions suggest intramolecular hydrogen bonding ($O{-}H\cdot\cdot O$) [17] as shown in figure 1.

Table 1. Analytical and physical data of H_2APNH and its metal complexes.

Compound	Empirical formula (F. Wt.)	Color	M.P. (°C)	Yield (%)	% Found (Calcd)				Λ_m*
					C	H	M	X	
H_2APHNH	$C_{18}H_{15}O_2N_3$ (305.321)	Yellow	245	80	69.87 (70.70)	4.84 (4.90)	–	–	–
$[Ni(H_2APHNH)Cl_2(H_2O)_2]\cdot H_2O$	$NiC_{18}H_{21}O_5N_3Cl_2$ (488.985)	Green	>300	75	44.25 (44.21)	4.36 (4.33)	11.89 (12.00)	14.61 (14.50)	6
$[Cd(H_2APHNH)Cl_2(H_2O)_2]\cdot H_2O$	$CdC_{18}H_{21}O_5N_3Cl_2$ (542.675)	Yellow	295	75	39.80 (39.83)	3.89 (3.90)	20.75 (20.71)	13.09 (13.06)	6
$[Co(H_2APHNH)Cl_2]$	$CoC_{18}H_{15}O_2N_3Cl_2$ (435.157)	Green	>300	70	49.70 (49.68)	3.39 (3.47)	13.45 (13.54)	16.31 (16.29)	5
$[Zn(H_2APHNH)Cl_2]$	$ZnC_{18}H_{15}O_2N_3Cl_2$ (441.597)	Orange	290	78	49.15 (49.11)	3.43 (3.42)	14.78 (14.80)	16.31 (16.29)	6
$[Hg(H_2APHNH)Cl_2]$	$HgC_{18}H_{15}O_2N_3Cl_2$ (576.817)	Yellow	290	80	37.51 (37.48)	2.80 (2.62)	12.33 (12.29)	34.90 (34.77)	6
$[Cd(H_2APHNH)(SO_4)]$	$CdC_{18}H_{15}O_6N_3S$ (513.781)	Yellow	>300	75	42.12 (42.08)	3.10 (2.94)	21.85 (21.87)	18.66 (18.69)	5
$[Ni(HAPHNH)_2]$	$NiC_{36}H_{28}O_4N_6$ (667.336)	Orange	>300	80	64.71 (65.79)	4.20 (4.23)	8.82 (8.79)	–	4
$[Zn(HAPHNH)_2]$	$ZnC_{36}H_{28}O_4N_6$ (673.996)	Yellow	295	80	64.08 (64.15)	4.15 (4.18)	9.69 (9.69)	–	4
$[UO_2(HAPHNH)_2(H_2O)_2]$	$UC_{36}H_{32}O_6N_3$ (914.658)	Orange	>300	70	47.34 (47.27)	3.45 (3.52)	26.21 (26.02)	–	3
$[Co(HAPHNH)_2]\cdot 2H_2O$	$CoC_{36}H_{32}O_6N_6$ (703.588)	Yellow	>300	75	61.48 (61.45)	4.51 (4.58)	8.29 (8.37)	–	4
$[Cu(HAPHNH)(OAc)(H_2O)]$	$CuC_{20}H_{19}O_6N_3$ (444.915)	Green	>300	70	53.72 (53.99)	4.30 (4.30)	14.19 (14.28)	–	3
$[Cu(HAPHNH)Cl]$	$CuC_{18}H_{14}O_2N_3Cl$ (403.306)	Green	295	70	53.62 (53.60)	3.66 (3.49)	15.82 (15.75)	8.81 (8.79)	4

X = Cl^- or SO_4^{2-}, * in DMSO ($ohm^{-1}\,cm^2\,mol^{-1}$).

Comparison of the IR spectrum of ligand and metal complexes (table 2) reveals that H_2APHNH is a bidentate, tridentate and/or tetradentate ligand depending on the metal salt and the reaction conditions.

In $[Ni(H_2APHNH)Cl_2(H_2O)_2] \cdot H_2O$, $[Cd(H_2APHNH)Cl_2(H_2O)_2] \cdot H_2O$ and $[Co(H_2APHNH)Cl_2]$ (figure 2), H_2APHNH is a neutral bidentate ligand coordinating via carbonyl oxygen (C=O) and azomethine nitrogen (C=N). This mode of complexation is supported by the shift of both υ(C=N) and υ(C=O) to lower wavenumbers. The υ(NH) remains more or less at the same position. The $\upsilon(OH)_{naphthoic}$ is shifted to a higher wavenumber. The IR spectra of these complexes show new bands in the 520–560, 370–380 and 270–290 cm^{-1} regions assignable to υ(M–O), υ(M–N) and υ(M–Cl) [18], respectively.

IR spectra of $[Zn(H_2APHNH)Cl_2]$ and $[Hg(H_2APHNH)Cl_2]$ show H_2APHNH as a neutral bidentate ligand coordinating through the azomethine nitrogen (C=N) and pyridyl nitrogen $(C{=}N)_{py}$, supported by the shifts of υ(C=N) to lower wavenumber and $\upsilon(C{=}N)_{py}$ to higher wavenumber. New bands in the 530–560 and 410–415 cm^{-1} regions are attributable to υ(M–O) and υ(M–N) [18], respectively. In the ^{1}H NMR spectrum of $[Zn(H_2APHNH)Cl_2]$ signals attributed to NH and OH remain at the same positions (10.87 and 12.21 ppm), indicating that these groups play no part in coordination.

H_2APHNH is a neutral tetradentate ligand in $[Cd(H_2APHNH)(SO_4)]$ coordinating via the $(OH)_{naphthoic}$, carbonyl oxygen (C=O), azomethine nitrogen $(C{=}N)_{hydrazone}$ and pyridyl nitrogen $(C{=}N)_{py}$. This mode of complexation is supported by shifts of $\upsilon(OH)_{naphthoic}$, υ(C=O) and $\upsilon(C{=}N)_{hydrazone}$ to lower wavenumbers while $\upsilon(C{=}N)_{py}$ is observed at a higher wavenumber. New bands observed at 512 and 405 cm^{-1} are tentatively assigned to υ(Cd–O) and υ(Cd–N) [18]. Bands at 1088 and 913 cm^{-1} assignable to the SO stretching vibrations suggest bidentate sulfate.

In $[Ni(HAPHNH)_2]$, $[Zn(HAPHNH)_2]$ and $[UO_2(HAPHNH)_2(H_2O)_2]$, H_2APHNH is mononegative bidentate coordinating via the azomethine nitrogen (C=N) and the deprotonated enolized carbonyl group ($=C–O^-$), forming two five-membered rings including the metal; the Ni(II) complex is shown in Supplemental Material. This complexation is supported by the disappearance of both υ(C=O) and υ(NH) with simultaneous appearance of new bands at 1636–1640 and 1167–1170 cm^{-1} assignable to υ(C=N*) [13] and enolic υ(C–O) [19], the negative shift of υ(C=N) and the appearance of new bands at 510–530 and 400–410 cm^{-1} tentatively assigned to υ(M–O) and υ(M–N) [18], respectively. The absence of a signal due to NH of the diamagnetic nickel(II) complex emphasizes the deprotonation of the enolized carbonyl oxygen ($=C–O^-$).

H_2APHNH is a mononegative tridentate ligand coordinating through the azomethine nitrogen (C=N), enolic oxygen ($=C–O^-$) and pyridyl nitrogen $(C{=}N)_{py}$ in $[Co(HAPHNH)_2] \cdot 2H_2O$, $[Cu(HAPHNH)_2(OAc)(H_2O)]$ and [Cu(HAPHNH)Cl], based on disappearance of υ(C=O) and υ(NH) with simultaneous appearance of new bands in 1634–1639 and 1160–1165 cm^{-1} regions assignable to υ(C=N*) and enolic υ(C–O), negative shift of υ(C=N), positive shift of $\upsilon(C{=}N)_{py}$ and appearance of new bands at 520–550 and 400–410 cm^{-1}. The copper(II) complex shows bands at 1460 and 1560 cm^{-1} attributable to the υ_s(O–C–O) and υ_{as}(O–C–O) of the acetate group. The difference (100 cm^{-1}) between those two bands indicates bidentate acetate [20].

Complexes with coordinated water were indicated by two bands at 875–877 and 768–776 cm^{-1} assigned to $\rho_r(H_2O)$ and $\rho_w(H_2O)$ [21] vibrations, respectively.

Table 2. Most important IR spectral bands of H_2APHNH and its metal complexes.

Compound	υ(OH) naphthoic	υ(NH)	υ(C=O)	υ(C=N)	$\upsilon(C{=}N)_{py}$	υ(C=N*)	υ(C–O) naphthoic	υ(C–O) enolic	υ(M–O)	υ(M–N)
H_2APHNH	3343	3261	1660	1640	610	–	1270		–	–
[Ni(H_2APHNH)Cl_2(H_2O)$_2$]H_2O	3449	3242	1633	1610	610	–	1268		520	370
[Cd(H_2APHNH)Cl_2(H_2O)$_2$]H_2O	3542	3234	1639	1614	606	–	1270		550	370
[Co(H_2APHNH)Cl_2]	3443	3214	1634	1615	610	–	1267		560	380
[Zn(H_2APHNH)Cl_2]	3575	3244	1657	1623	618	–	1273		560	410
[Hg(H_2APHNH)Cl_2]	3543	3202	1659	1622	618	–	1270		530	415
[Cd(H_2APHNH)(SO_4)]	3267	3148	1643	1618	623	–	1271		512	405
[Ni(HAPHNH)$_2$]	3445	–	–	1596	610	1640	1272	1170	530	404
[Zn(HAPHNH)$_2$]	3451	–	–	1592	608	1636	1270	1169	520	410
[UO_2(HAPHNH)$_2$(H_2O)$_2$]	3506	–	–	1578	610	1639	1273	1167	510	400
[Co(HAPHNH)$_2$] · $2H_2O$	3444	–	–	1593	619	1634	1270	1165	520	400
[Cu(HAPHNH)(OAc)(H_2O)]	3562	–	–	1600	626	1639	1269	1160	520	400
[Cu(HAPHNH)Cl]	3455	–	–	1598	618	1639	1263	1161	550	410

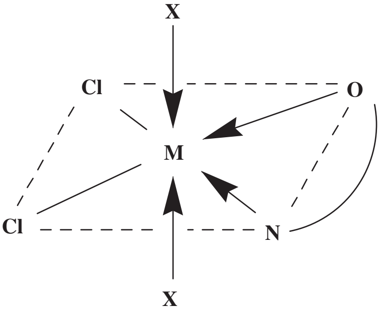

M = Ni(II) and Cd(II); X = H_2O

M = Co(II); X = 0

Figure 2. Chelation of $[Ni(H_2APHNH)Cl_2(H_2O)_2]H_2O$, $[Cd(H_2APHNH)Cl_2(H_2O)_2]H_2O$ and $[Co(H_2APHNH)Cl_2]$.

The IR spectrum of $[UO_2(HAPHNH)_2(H_2O)_2]$ has bands at 920, 870 and 268 cm^{-1} assigned to υ_3, υ_1 and υ_4 vibrations, respectively, of the dioxouranium ion. The υ_3 can be used to calculate the force constant (F) of υ(U=O) by the method of McGlynn *et al.* [22].

$$(\upsilon_3)^2 = (1307)^2(F_{U-O})/14.103$$

The force constant obtained was then substituted into the relation given by Jones [23] to give an estimate of the (U–O) bond length in Å.

$$R_{U-O} = 1.08(F_{U-O})^{-1/3} + 1.17$$

The calculated F_{U-O} and R_{U-O} values are 6.987 m dynes $Å^{-1}$ and 1.735 Å, respectively, in the usual range for uranyl complexes.

Complexes of H_2APHNH and Ni(II), Co(II), Cu(II), Zn(II), Cd(II), Hg(II) and $U(VI)O_2$ from the same technique have different modes of coordination. In Ni(II), Co(II), Zn(II), Cd(II) and Hg(II) chloride complexes, H_2APHNH is neutral bidentate, while in Cu(II) chloride, Cu(II) and Co(II) acetate are mononegative tridentate but for Ni(II), Zn(II) and $U(IV)O_2$ acetate complexes, H_2APHNH is mononegative bidentate. The ligand is tetradentate with Cd(II) sulfate.

3.2. *Electronic, ESR spectra and magnetic moment measurements*

Magnetic moments, electronic spectral bands in DMSO and ligand field parameters of the metal complexes are in table 3. The diamagnetic behavior of $[Ni(HAPHNH)_2]$ indicates a square planar configuration. Furthermore, the electronic spectrum shows a characteristic band at 18182 cm^{-1} assigned to $^1A_{1g} \rightarrow {}^1A_{2g}$ in a square planar geometry [24]. The electronic spectrum of $[Ni(H_2APHNH)Cl_2(H_2O)_2] \cdot H_2O$ shows two bands at 13605 and 24380 cm^{-1} attributed to $^3A_{2g} \rightarrow {}^3T_{1g}(F)$ and $^3A_{2g} \rightarrow {}^3T_{1g}(P)$ transitions, respectively, in an octahedral geometry [25]. The calculated values of D_q, B, β and υ_2/υ_1 lie in the range reported for octahedral structures. The position of υ_1 (8146 cm^{-1}) is calculated theoretically. The magnetic moment value ($\mu_{eff} = 3.40$ B.M.) is additional evidence for octahedral geometry.

Table 3. Magnetic moments, electronic spectra and ligand field parameters of metal complexes of H_2APHNH.

Compound	$\mu_{eff.}$ (B.M.)	Band position (cm^{-1})	D_q (cm^{-1})	B (cm^{-1})	β	υ_2/υ_1
$[Ni(H_2APHNH)Cl_2(H_2O)_2] \cdot H_2O$	3.40	13605; 24380	903	813	0.87	1.67
$[Ni(HAPHNH)_2]$	Diam.	18182	–	–	–	–
$[Co(H_2APHNH)Cl_2]$	4.38	14705; 16529	–	–	–	–
$[Co(HAPHNH)_2] \cdot 2H_2O$	5.15	14211; 17212	766	766	0.79	2.15
$[Cu(HAPHNH)(OAc)(H_2O)]$	2.18	14815; 16000	–	–	–	–
$[Cu(HAPHNH)Cl]$	1.82	14454	–	–	–	–
$[UO_2(HAPHNH)_2(H_2O)_2]$	Diam.	23980; 27855	–	–	–	–

Table 4. ESR data of the copper(II) complexes at room temperature.

Complex	$g_{\parallel}$	$g_{\perp}$	$A_{\parallel}$* (cm^{-1})	G	$g_{\parallel}/A_{\parallel}$	α^2	β^2	Symm.
$[Cu(HAPHNH)Cl]$	2.40	2.09	180	4.4	133	0.97	0.89	D_{4h}
$[Cu(HAPHNH)(OAc)(H_2O)]$	2.28	2.06	165	4.6	138	0.8	0.77	O_h

The electronic spectrum of $[Co(HAPHNH)_2] \cdot 2H_2O$ exhibits bands at 14211 and 17,212 cm^{-1} attributed to $^4T_{1g} \rightarrow {}^4A_{2g}(F)$ and $^4T_{1g} \rightarrow {}^4T_{1g}(P)$, respectively, in an octahedral configuration [25]. The calculated D_q, B, β and υ_2/υ_1 values are in the range reported for an octahedral environment around Co(II). The position of υ_1 (6609 cm^{-1}) is calculated [25]. The magnetic moment (5.15 B.M.) is additional evidence for octahedral geometry around Co(II). The electronic spectrum of $[Co(H_2APHNH)Cl_2]$ exhibits one main band at 14,705 cm^{-1} attributed to $^4A_2 \rightarrow {}^4T_1(P)$. There is also a shoulder at 16,529 cm^{-1} due to spin-orbit coupling. The magnetic moment (4.38 B.M.) is evidence for a tetrahedral geometry around the Co(II) ion [25].

The copper(II) complexes have magnetic moment values (1.82–2.18 B.M.) which correspond to those reported for d^9-systems. The electronic spectrum of [Cu(HAPHNH)Cl] exhibits a broad band with a maximum at 14,454 cm^{-1} assigned to $^2B_{1g} \rightarrow {}^2A_{1g}$ for square planar Cu(II) [25]. The electronic spectrum of $[Cu(HAPHNH)(OAc)(H_2O)]$ complex shows a broad band at 16,000 cm^{-1} with a shoulder at 14815 cm^{-1} assigned to $^2B_{1g} \rightarrow {}^2E_g$ and $^2E_g \rightarrow {}^2A_{1g}$ transitions, respectively, in a tetragonally distorted octahedral configuration [26].

The electronic spectrum of $[UO_2(HAPHNH)_2(H_2O)_2]$ shows bands at 23,980 and 27,855 cm^{-1} may be ascribed to $^1\Sigma_g^+ \rightarrow {}^2\pi_u$ transition for dioxouranium(VI) and charge transfer $n \rightarrow \pi^*$, respectively [27].

The solid state ESR spectra exhibit axially symmetric g-tensor parameters with $g_{\parallel} > g_{\perp} > 2.0023$ indicating that the copper site has a $d_{x^2-y^2}$ ground-state [28]. The spin Hamiltonian parameters of these complexes were calculated (table 4). In axial symmetry the g-values are related by the expression $G = (g_{\parallel} - 2)/(g_{\perp} - 2) = 4$, where G is the exchange interaction parameter. According to Hathaway [29], if the value of G is greater than 4, the exchange interaction between copper(II) centers in the solid state is negligible, whereas less than 4 indicates a considerable exchange interaction. The calculated G values $(G = (g_{\parallel} - 2)/(g_{\perp} - 2) = 4)$ for $[Cu(HAPHNH)(OAc)(H_2O)]$

and [Cu(HAPHNH)Cl] are 4.6 and 4.4, respectively, suggesting no copper-copper exchange interactions.

The tendency of $A_{\|}$ to decrease with an increase of $g_{\|}$ is an index of increasing of tetrahedral distortion in the coordination sphere of copper [30]. In order to quantify the degree of distortion of the copper(II) complexes, we selected the f factor $g_{\|}/A_{\|}$ obtained from the ESR spectra, which is considered as an empirical index of tetrahedral distortion [31]. It ranges between 105 and 135 for square-planar complexes, depending on the nature of the coordinated atoms; a tetrahedrally-distorted structure can have much larger values [32]. For [Cu(HAPHNH)Cl] the $g_{\|}/A_{\|}$ quotient is 133, supporting square-planar geometry with no appreciable tetrahedral distortion. The ratio $g_{\|}/A_{\|}$ for [Cu(HAPHNH)(OAc)(H_2O)] is 138, demonstrating significant dihedral angle distortion in the *xy*-plane and tetrahedral distortion from square-planar geometry.

Superhyperfine structure for this complex was not seen at higher fields excluding any interaction of the nuclear spins of nitrogen ($I = 1$) with the unpaired electron density on Cu(II).

Molecular orbital coefficients, α^2 (covalent in-plane σ-bonding) and β^2 (covalent in-plane π-bonding), were calculated [33–36]:

$$\alpha^2 = -(A_{\|}/0.036) + (g_{\|} - 2.0023) + 3/7(g_{\perp} - 2.0023) + 0.04$$

$$\beta^2 = (g_{\|} - 2.0023)\mathrm{E}/ - 8\lambda\alpha^2$$

$\lambda = 828\ \mathrm{cm}^{-1}$ for the free ion and E is the $^2\mathrm{B}_{1g} \rightarrow {}^2\mathrm{A}_{1g}$ transition

In-plane σ-bonding $\alpha^2 = 1$ indicates complete ionic character, whereas $\alpha^2 = 0.5$ denotes 100% covalent bonding, with the assumption of negligibly small values of the overlap integral. The β^2 parameter gives an indication of the covalency of the in-plane π-bonding. The smaller β^2, the larger the covalency of the bonding.

The values of α^2 and β^2 for [Cu(HAPHNH)(OAc)(H_2O)] indicate that the in-plane σ-bonding and in-plane π-bonding are appreciably covalent and are consistent with very strong in-plane π-bonding, but in [Cu(HAPHNH)Cl], the results indicate that the in-plane σ-bonding and in-plane π-bonding are appreciably ionic. These results are anticipated because there are appropriate ligand orbitals to combine with the d_{xy} orbital of copper(II). For square-planar geometry complexes, lower values of β^2 compared to α^2 indicate that the in-plane π-bonding is more covalent than the in-plane σ-bonding. These data are consistent with reported values [37–40].

3.3. *Thermal analysis*

The TG and DTG curves of [Ni(HAPHNH)$_2$] show that it is thermally stable up to 377°C, above which decomposition of the complex begins. In the temperature range 377–433°C, the TG curve displays 42.9% weight loss (Supplementary Material) which could be ascribed to elimination of two loosely bound 3-hydroxynaphthoyl ($C_{10}H_7O$) moieties. The second weight loss stage (433–508°C) is largely due to full decomposition of the remaining organic portions ($2C_8H_7N_3$) of the ligands as well as the release of half an oxygen. This stage is accompanied by 46.0% weight loss in the TG curve. The final product is NiO at 11.1%.

The TG curves of [Cd(H_2APHNH)Cl_2(H_2O)$_2$]$\cdot H_2O$ display 3.3% weight loss in the temperature range 84–126°C which correlate to one water outside the

Table 5. Thermal behavior of Ni(II) and Cd(II) complexes of H_2APHNH.

			Wt. Loss%	
Complex	Temp. range (°C)	Decomp. prod. (Formula Wt.)	Found	Calcd
[Ni(HAPHNH)$_2$]	377–433	$2C_{10}H_7O$ (286.312)	42.9	42.9
	433–508	$2C_8H_7N_3+\frac{1}{2}O_2$ (306.33)	46.0	45.9
	>508	Residue, NiO (74.71)	11.1	11.2
[Cd(H_2APHNH)$Cl_2(H_2O)_2$] · H_2O	84–126	H_2O (18.016)	3.3	3.3
	250–331	$2H_2O$ (36.032)	6.7	6.6
	331–400	Cl_2 (70.906)	13.0	13.1
	468–622	$C_{10}H_7O$ (143.156)	26.5	26.4
	622–718	$C_8H_8N_3$ (146.173)	26.8	26.9
	>718	Residue, CdO (128.400)	23.7	23.7

coordination sphere. In the temperature range 250–331°C, the TG curves exhibit 6.7% weight loss ascribed to elimination of two coordinating waters [41]. In the temperature range 331–400°C, the TG curve displays 13.0% weight loss corresponding to release of chlorine [41]. Thermal degradation of the organic molecule starts above 468°C. Over the temperature range 468–622°C, the weight loss 26.5% in the TG curve is assigned to elimination of loosely bound 3-hydroxy naphthyl ($C_{10}H_7O$). The final weight loss of 26.8% ending at 718°C is attributed to complete decomposition of the remaining organic molecules, with rupture of the chelate bond, leaving CdO (23.7%). Kinetics of the thermal decompositions are presented in the Supplementary Material. Thermal analyzes are given in table 5.

3.4. *Antimicrobial activity bioassay*

The antimicrobial activities of ligand and complexes against *B. Subtillis* and *P. Aeurginosa* are summarized in table 6. Growth inhibition zones are proportional to the antimicrobial activity of the tested compound. The data suggest that Gram-positive and Gram-negative bacteria were affected by the tested chemicals with strongest activity for the ligand, copper, mercury and cadmium complexes.

3.5. *Eukaryotic DNA degradation test*

Examination of the electrophoretic mobility (Supplementary Material) in comparison to the control sample revealed change in lane 1, high downward shifts in mobility in lanes 2, 3, and 4, associated with tailing of the DNA. Electrophoretic mobility shift and tailing of DNA in any lane are indicative of degradation of calf thymus DNA. DNA degradation and antimicrobial activity against Gram-positive and Gram-negative bacteria coincided. The degradation powers of the tested chemicals on calf thymus DNA were high, supporting selective action of these compounds against bacteria and the human or related eukaryotic organism.

Table 6. Inhibited zones diameter (I. Z. D.) in mm as a criterion of antibacterial activity of the ligands and its complexes at concentration level of 2 mg mL^{-1}.

	Bacteria	
	B. Subtillis (G. +ve)	*P. Aeurginosa* (G. –ve)
Compounds	I. Z. D. (mm)	I. Z. D. (mm)
H_2APHNH	25	25
[Ni(HAPHNH)$_2$]	12	12
[Co(HAPHNH)$_2$]	12	12
[Cu(HAPHNH)(OAc)(H_2O)]	27	30
[Zn(HAPHNH)$_2$]	18	12
[Hg(H_2APHNH)Cl_2]	35	35
[Cd(H_2APHNH)Cl_2(H_2O)$_2$]	36	36
[UO_2(HAPHNH)$_2$(H_2O)$_2$]	18	12

References

[1] M.E. Khalifa. *Analysis Fr.*, **23**, 453 (1995).
[2] Y.P. Kitaev, B.I. Buzykin, T.V. Troepolskaya. *Russ. Chem. Rev.*, **39**, 441 (1970).
[3] A. Panico, P. Vicini, M. Incert, V. Cardile, B. Gentile, G. Ronsisvalle. *II Farmaco*, **57**, 671 (2002).
[4] P. Sienkiewich, K. Bielawski, A. Bielawska, J. Palka. *Environ. Toxicol. Pharmacol.*, **20**, 118 (2005).
[5] A. Bielawska, K. Bielawski, A. Muszynska. *II Farmaco*, **59**, 111 (2004).
[6] T.M. Sielecki, J. Liu, S.A. Mousa, A.L. Racanelli, E.A. Hausner, R.R. Wexler, R.E. Olson. *Bioorg. Med. Chem. Lett.*, **11**, 2201 (2001).
[7] J.W. Liebeschuetz, S.D. Jones, P.J. Morgan, C.W. Murray, A.D. Rimmer, J.M.E. Roscoe, B. Waszkowycz, P.M. Welsh, W.A. Wylie, S.C. Young, H. Martin, J. Mahler, L. Brady, K. Wilkinson. *J. Med. Chem.*, **45**, 1221 (2002).
[8] M. Bakir, I. Hassan, T. Johnson, O. Brown, O. Green, C. Gyles, M.D. Coley. *J. Mol. Struct.*, **688**, 213 (2004).
[9] A. El-Dissouky, O. Al-Fulij, S.S. Kandil. *J. Coord. Chem.*, **57**, 605 (2004).
[10] A.I. Vogel. *Quantitative Inorganic Analysis*, Longmans, London (1989).
[11] P. Gerhardt. *Manual of Methods for General Bacteriology*, American Society for Microbiology, Castello (1981).
[12] M.M. Mostafa, M.A. Khattab, K.M. Ibrahim. *Polyhedron*, **2**, 583 (1983).
[13] F.B. Tamboura, P.M. Haba, M. Gaye, A.S. Sall, A.H. Barry, T. Jouini. *Polyhedron*, **23**, 1191 (2004).
[14] D.X. West, C.S. Carlson, A.C. Whyte. *Transition Met. Chem.*, **15**, 43 (1990).
[15] C. Dongli, J. Handong, Z. Hongyun, C. Deji, Y. Jina, L.B. Jian. *Polyhedron*, **13**, 57 (1994).
[16] R. Gup, B. Kirkan. *Spectrochim. Acta A*, **62**, 1188 (2005).
[17] D.X. West, L.D. Borowy. *Transition Met. Chem.*, **16**, 5 (1991).
[18] D.X. West, D.L. Huffman. *Transition Met. Chem.*, **14**, 190 (1989).
[19] T.H. Rakha, N. Nawar, G.M. Abu El-Reach. *Synth. React. Inorg. Met.-Org. Chem.*, **26**, 1705 (1996).
[20] K.M. Ibrahim, M.M. Bekheit. *Transition Met. Chem.*, **13**, 230 (1988).
[21] K. Nakamoto. *Infrared Spectra of Inorganic and Coordination Compounds*, Wiley, New York (1970).
[22] S.P. McGlynn, J.K. Smith. *J. Chem. Phys.*, **35**, 105 (1961).
[23] H. Jones. *Spectrochim. Acta A*, **10**, 395 (1958).
[24] S. Singh, B.P. Yadava, R.C. Aggarwal. *Ind. J. Chem.*, **23A**, 441 (1984).
[25] A.B.P. Lever. *Inorganic Electronic Spectroscopy*, Elsevier, Amsterdam (1968).
[26] L. Sacconi. *Transition Met. Chem.*, **4**, 199 (1979).
[27] R.G. Bhattacharya, D.C. Bera. *J. Ind. Chem. Soc.*, **52**, 373 (1975).
[28] G. Speier, J. Csihony, A.M. Whalen, C.G. Pierpont. *Inorg. Chem.*, **35**, 3519 (1996).
[29] B.J. Hathaway, D.E. Billing. *Coord. Chem. Rev.*, **5**, 143 (1970).
[30] J.L. Mesa, J.L. Pizarro, M.I. Arriortua. *Cryst. Res. Technol.*, **33**, 3 (1998).
[31] V.T. Kasumo. *Spectrochim. Acta A*, **57**, 1649 (2001).
[32] J.A. Wellman, F.B. Hulsbergen. *J. Inorg. Nucl. Chem.*, **40**, 143 (1978).
[33] R.K. Ray, G.R. Kauffman. *Inorg. Chim. Acta*, **173**, 207 (1990).

[34] K. Jayasubramanian, S.A. Samath, S. Thambidurai, R. Murugesan, S.K. Ramalingam. *Transition Met. Chem.*, **20**, 76 (1995).

[35] V.S.X. Anthonisamy, R. Murugesan. *Chem. Phys. Lett.*, **287**, 353 (1998).

[36] V.S.X. Anthonisamy, R. Anantharam, R. Murugesan. *Spectrochim. Acta A*, **55**, 135 (1999).

[37] N. Raman, Y.P. Raja, A. Kulandaisamy. *Proc. Indian Acad. Sci. (Chem. Sci.)*, **113**, 183 (2001).

[38] R.P. John. *Spectrochim. Acta A*, **59**, 1349 (2003).

[39] G.A.A. Al-Hazmi, M.S. El-Shahawi, E.M. Gabr, A.A. El-Asmy. *J. Coord. Chem.*, **58**, 713 (2005).

[40] N.M. El-Metwally, I.M. Gabr, A.A. Abou-Hussen, A.A. El-Asmy. *Transition Met. Chem.*, **31**, 71 (2006).

[41] T.H. Rakha, K.M. Ibrahim, M.E. Khalifa. *Thermochim. Acta*, **144**, 53 (1989).